

Molecular Dynamics Studies of the Conformational Preferences of a DNA Double Helix in Water and an Ethanol/Water Mixture: Theoretical Considerations of the A \rightleftharpoons B Transition

D. Sprous, M. A. Young, and D. L. Beveridge*

Chemistry Department and Molecular Biophysics Program, Wesleyan University,
Middletown, Connecticut 06459-0180

Received: December 17, 1997; In Final Form: March 18, 1998

A series of molecular dynamics (MD) computer simulations were carried out to explore the conformational preferences of a dynamic model of the sodium salt of the DNA duplex d(CGCGAATTCGCG) in water and in a mixed solvent comprised of 85% (v/v) ethanol/water. This sequence is observed to assume a B-form structure in the solid state and in aqueous solution and is expected to assume an A-form structure in the mixed solvent environment. The MD simulations are based on the empirical force field proposed recently by Cornell et al.¹ and carried out with long-range interactions treated via the particle mesh Ewald method using the AMBER 4.1 modeling package.^{2–4} This study builds on the results of a previous 5 ns MD simulation on d(CGCGAATTCGCG) in water,⁵ now extended to 13 ns, which resulted in a well-stabilized B-form dynamical structure. Three additional simulations are reported: one simulation starts from the A-form in water, the second starts from the A-form in 85% (v/v) ethanol/water, the last starts from the B-forms in 85% (v/v) ethanol/water. The MD on the A-form structure in water undergoes an A- to B-DNA transition and stabilizes in the B-form. The corresponding 2.0 ns MD in ethanol/water remains an A-form structure, as expected. However, the B-form structure in the 85% (v/v) ethanol/water remains B-form even after 2.0 ns of MD, contrary to expectation. Comparisons of our results with those of parallel studies based on AMBER and pertinent results obtained using other current force fields are provided, and the use of conformational preferences as a performance index for nucleic acids force fields is discussed.

Introduction

A series of molecular dynamics computer simulations have been carried out to explore the conformational preferences of a dynamical model of the DNA duplex d(CGCGAATTCGCG) in water and in a mixed solvent comprised of 85% (v/v) ethanol and 15% (v/v) water. This particular sequence is observed to assume a B-form structure in the crystalline state^{6–11} and in aqueous solution¹² and is expected to assume an A-form structure in the mixed solvent.^{13,14} The B-form is predominant at physiological conditions,^{13,15} but RNA/DNA hybrids, a natural consequence of DNA transcription, can be expected to show a mix of B- and A-form quality.^{16,17} DNA sequences complexed to proteins can be A- or B-form and exhibit B/A junctions.^{18,19} Thus, an accurate description of the A/B conformational preferences of DNA sequences is expected to be important in modeling studies applied to DNA-related problems in structural biology.

The MD simulations in the current study are based on the empirical force field proposed recently by Cornell et al.,¹ which includes specific improvements in parameters for describing nucleic acids in solution. All MD was performed using the AMBER 4.1 suite of programs with long-range interactions treated via the particle-mesh Ewald method.^{2–4} In a prior study of d(CGCGAATTCGCG) in water,⁵ MD starting with either the canonical B or crystal structure of the sequence or with three alternative initial placements of Na⁺ ions stabilized at a B-form structure on the nanosecond time scale. In the present study, the preceding result is considered with those from three new

and related nanosecond simulations: one with a starting configuration of A-form DNA in water, and two more, both in 85% (v/v) ethanol/water mixed solvent, with starting configurations of A- and B-form DNA, respectively. We compare our results with those of parallel studies based on AMBER^{20,21} and MD studies based on other current force fields.^{22–24} The question addressed in this study is how well the assumed force field and simulation protocol support expected conformational preferences on a well-characterized full turn of the DNA double helix.

Background

The A-DNA form is stable in fiber samples maintained at a relatively low level of (<76%) relative humidity, while B-DNA is the preferred form at higher relative humidity (>86%).¹⁷ Ivanov and co-workers,^{13,15} showed that preferential stability of A- and B-forms of calf thymus DNA in solution is strictly a function of water activity, with the B-form favored under conditions of high water activity (aqueous solutions) and the A-form stabilized under low water activity. Low water activity conditions can be induced by adding aliphatic alcohols such as ethanol or can be induced by molar concentrations of chaotropic salt solutions.^{13,15} For calf thymus DNA, the characteristic CD signature for A-DNA is reached by 75% ethanol concentrations.¹³ The influence of base pair sequence on conformational preference has been delineated empirically;¹⁴ sequences of G and C base pairs have a propensity toward A-form structures and the introduction of A and T residues introduces conformation fluidity and an ability to undergo an A to B interconversion as a function of water activity. These observations now provide

* Corresponding author: dbeveridge@wesleyan.edu.

a basis for assessing the performance of all-atom MD simulations of DNA including water and counterions.

Dynamical models of DNA sequences in solution obtained from MD simulation provide a detailed microscopic description of molecular structure and motions.^{25,26} The accuracy and general applicability of MD models of DNA depend on the quality of the empirical force field used to determine the configurational energies and forces. A series of force fields have been utilized in MD simulations on DNA in recent years, and while a measure of success was achieved in some cases, in others the MD did not support reasonably stable forms of the B-DNA double helix in aqueous solution.²⁷ The problems originate mainly in the force fields, as ad hoc modifications were shown to improve the results. An ability to support the A-DNA form under low water activity conditions and the B-DNA form under high water activity conditions is an important trait for a force field used for nucleic acids.

Recently, extensive research efforts have been applied to developing improved MD force fields including parameter revisions designed specifically for the simulation of nucleic acids in solution.^{1,28} In particular, a new all-atom MD force field was proposed by Cornell et al.¹ and incorporated into the AMBER 4.1 suite of programs.²⁻⁴ MD models of B-form DNA oligonucleotides in water based on this force field have been reported by Kollman and co-workers on the decamer d(C-CAACGTTGG)^{20,21} and by Duan et al.²⁹ and Young et al.⁵ on d(CGCGAATTCGCG). In the latter study, MD starting with either the canonical B-form or crystal structure of the sequence and three alternative initial placements of Na⁺ ions resulted in a well-stabilized B-form DNA after 5 ns of MD, now extended to 13 ns. Cheatham et al.^{20,21} reported that the expected A/B conformational preferences were observed for d(CCAACGTTGG) in water, including an A- to B-DNA transition. However, in a solution of 85% (v/v) ethanol/water, a simulation beginning in the B-form did not make the expected conformational transition to the A-form.²¹ Modification of a single dihedral force constant in the sugars enabled the MD structure to convert to the A-form, but agreement on preferential stability of the B-form in water was compromised.²¹ A new CHARMM force field for nucleic acids was reported by MacKerell et al.²⁸ Simulations reported by MacKerell²³ and independent assessments^{22,24} indicate that this force field has a propensity for A-form structures independent of environmental condition. Indeed, simulations in the presence of Mg²⁺, which stabilizes B-DNA in experiment, undergo B- to A-DNA transitions within 1 ns²³ with the MacKerell et al. force field.²⁸

To fully test the fitness of a force field for simulation in regard to the issue of the A- and B-form equilibrium requires at minimum four simulations: first, B-DNA starting configuration in high water activity, which should be stable; second, A-DNA starting configuration in high water activity, which should convert to B-DNA; third, B-DNA starting configuration in low water activity, which should convert to A-DNA; and last, A-DNA starting configuration in low water activity, which should be stable. In Yang and Pettitt,²⁴ a corresponding study for high water activity was not considered; from other reports^{23,30} one would expect this to be an A-form structure as well, somewhat mitigating the significance of seeing a B to A transition in 400 mM salt.

As a computationally efficient prototype system to explore the technical issues involved in mixed solvent simulations, we investigated the conformational preferences of the hexameric sequence d(GCCGGC) in water and mixed 75% (v/v) ethanol/water via MD based on the Cornell et al. force field,¹ with a

TABLE 1: Systems Simulated and Their Initial DNA Form and Ethanol/Water Configuration

	shorthand tag for specific simulations	initial DNA form	number of waters	number of ethanols	ethanol/water configuration
case 1	12Bw	B	3949	0	
case 2	12Aw	A	3357	0	
case 3	12Ae-or	A	502	877	opls random
	12Ae-ob	A	502	877	opls biphasic
	12Ae-fr	A	502	877	Fox random
	12Ae-fb	A	502	877	Fox biphasic
case 4	12Be-or	B	502	877	opls biphasic

PME treatment of long-range interactions.^{3,4} The NaCl concentration was held at 100 mM throughout all four hexameric simulations, producing a net condition that should clearly favor A-DNA with the addition of the 75% (v/v) ethanol solution.^{13,15} This sequence is observed to adopt an A-form in the crystal.³¹ Four simulations were performed: B-DNA starting configuration in straight TIP3P-water; A-DNA starting configuration in straight TIP3P-water; B-DNA starting conformation in 75% (v/v) OPLS-ethanol/TIP3P-water; and last, A-DNA starting configuration in 75% (v/v) OPLS-ethanol/TIP3P-water. In the each of our four simulations, d(GCCGGC) assumed a B-form structure regardless of starting structure or solution condition, whereas the A-form is expected in the mixed ethanol/water solutions. The results on short oligomeric sequences may be susceptible to end effects, and in this MD the whole hexamer shows unwinding beyond 800 ps. By contrast, Cheatham et al.,²⁰ as described above, observed a stable A-form of d(C-CAACGTTGG) at low water activity, but used a higher concentration of an all-atom model of ethanol and a different solvent equilibration protocol. In the present study, we consider the d(CGCGAATTCGCG) duplex, in which a full turn of DNA is represented. We describe herein results of nanosecond MD simulations on the Eco RI dodecamer started from both the A- and B-canonical forms in both aqueous solutions and in an 85% (v/v) ethanol/water mixed solvent. Further issues and concerns in the parametrization of the ethanol model and equilibration protocols in MD simulations involving mixed solvent systems are also addressed and discussed.

Calculations

The AMBER utility NUCGEN was employed to create canonical A- and B-DNA starting structures for the d(CGCGAATTCGCG) duplex based on fiber diffraction structures.³² Phosphate moieties are assigned to the 5' residue, and thus each dodecamer strand contains 11 PO₄⁻ anions and the duplex carries a net charge of -22 eu. The 3' end of the sugar-phosphate backbone is terminated with OH groups. Electro-neutrality was established by adding 22 sodium cations to the system randomly about the DNA. Aqueous solutions were constructed with the addition of water molecules. The mixed solvent was configured at a concentration of 85% (v/v) ethanol/water. All MD simulations were performed in the TPN ensemble using AMBER 4.1³³ and the Cornell et al. force field¹ for nucleic acids and employ particle-mesh Ewald (PME)^{3,4} summation for long-range interactions. Water in the simulation was described using the TIP3P model.³⁴⁻³⁶ Two options for ethanol were considered, one based on the all-atom parametrization of Fox and Kollman³⁷ (FK-ethanol) and the other the united atom OPLS model (OPLS-ethanol).^{34-36,38} In Fox and Kollman,³⁷ the ethanol charges were assigned to reproduce the electrostatic potential determined at a HF/6-31G* level of theory

according to the RESP methodology.^{39,40} Both the FK-ethanol and OPLS-ethanol models closely approximate the correct density, heat capacity, and heat of vaporization observed for ethanol.^{37,38} However, the united atom OPLS-ethanol model is more computationally efficient: we observed that the d(CGCGAATTCGCG) sequence in 85% (v/v) OPLS-ethanol/TIP3P-water system requires 40% less computer time, a major saving in simulations of large dimensionality. The initial dimension of the simulation cell for d(CGCGAATTCGCG) was $45 \times 45 \times 60$ Å. Two starting configurations were considered in the mixed solvent case: first, ethanols and waters were positioned randomly in the prescribed box around the DNA (either the A- or B-forms) and associated Na^+ , and second, following Cheatham et al.,²⁰ a "biphasic" initial configuration constructed by first adding ethanols subject to the requirement that all added ethanol atoms be greater than 6 Å from the DNA. The process did incorporate waters in the ethanol-rich phase where space was adequate for an insertion. The systems studied are fully defined in Table 1.

The MD protocol of minimization, heating, equilibration, and production dynamics was carried out as follows: minimization was carried out with 150 steps of the steepest descent method followed by 350 steps of conjugate gradient minimization. On the first cycle, 25 kcal mol⁻¹ Å⁻² positional constraints were placed on the DNA. The constraints were dropped to 5 kcal mol⁻¹ Å⁻² for the additional four cycles. All MD was performed under constant pressure conditions. Other operational parameters were a 2 fs time step, a 9 Å cutoff for direct space nonbonded calculations, and a 0.000 01 convergence criteria for the Ewald portion of the nonbonded interactions. Heating from 0 to 300 K was done over 10 ps, followed by equilibration at 300 K for a total of 30 additional ps. Equilibration was assumed when the system energy was stable when coupled with a SHAKE constraint of 5×10^{-5} Å on all covalent bonds involving hydrogen atoms. Positional constraints were set initially to 25 kcal mol⁻¹ Å⁻², with a 5 kcal mol⁻¹ Å⁻² constraint held constant throughout the 30 ps equilibration protocol.

Analysis of the various trajectories was carried out using MD ToolChest.⁴¹ The key structural parameters in distinguishing A- and B-forms of DNA are the x-displacement and inclination of base pairs from the helix axis, XDP and INC, respectively, and the sugar puckers. For canonical B-form DNA, XDP = 0, INC = 0 and sugars are in the C2'-endo form. For A-DNA, XDP = -5.2 Å, INC = 20°, and the sugar rings are in the C3'-endo form.¹⁷ The distributions of XDP and INC found in oligonucleotide crystal structures differ slightly but significantly from canonical values; plots of these have been reported in the aforementioned article by Young et al.⁵

The distribution of the solvent species around the DNA was quantified using a proximity analysis based radial distribution function ($g(R)$) calculation^{42,43} for each of the following solvent atom species: water oxygen atoms, Na^+ atoms, ethanol oxygen atoms, and ethanol methyl carbon united atoms. The resulting proximity $g(R)$ data are comprised of solvent atom densities for concentric spherical shells of the solvent accessible volume around each individual solute atom. The reported densities are average values calculated over the entire trajectory. The proximity technique considers the total number of solvent atoms and the solvent accessible volume in each snapshot, partitioning these parameters among individual solute atoms. The $g(R)$ measures for groups of individual atoms can be combined to generate solvent $g(R)$ plots for entire groups of solute atoms, or even the entire solute. The final $g(R)$ plots for individual or

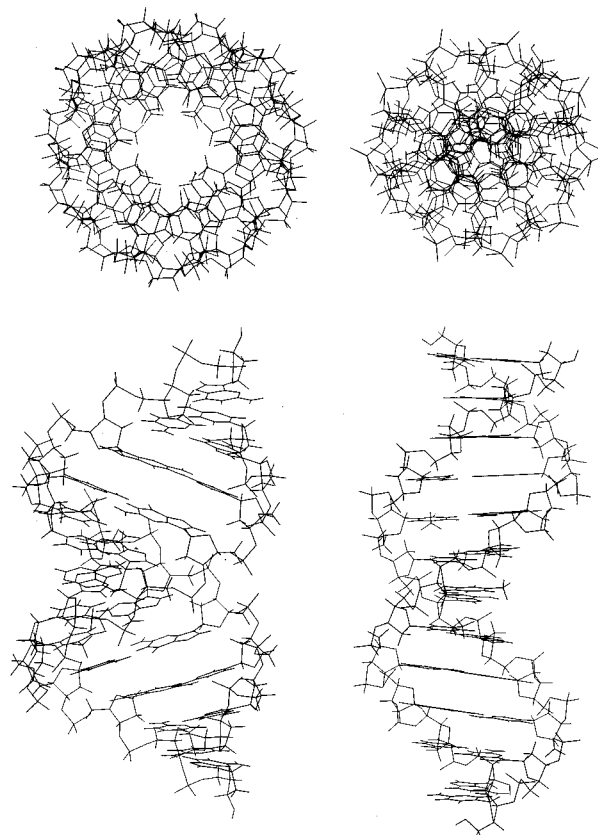


Figure 1. d(CGCGAATTCGCG) in its canonical A-DNA (left) and canonical B-DNA (right) forms.

combined groups of solute atoms are plotted on a probabilistic scale, calculated by normalizing the solvent densities relative to the bulk solvent density, calculated as the total number of each solvent atom species divided by the solvent-accessible volume of the simulation cell. The resulting probabilities will converge to unity at infinite R , where bulk solvent properties are observed.

Results

The four cases delineated in MD on d(CGCGAATTCGCG) are discussed in the following order: (1) starting structure B-form in water; (2) starting structure A-form in water; (3) starting structure A-form in 85% (v/v) ethanol/water; and 4) starting structure B-form in 85% (v/v) ethanol/water. Plots of root-mean-square deviation of the MD structures as functions of time against an A-canonical reference structure ($\text{rms}(A,t)$) and against a B-canonical reference structure ($\text{rms}(B,t)$) for each of the simulations are collected in Figure 2. After discussing each of the case simulations individually, we present a comparison of the solvent structure around the DNA for case 1 and case 3.

Case 1. Starting Structure B-Form in Water. This case has been dealt with previously in MD simulations from this laboratory described fully by Young et al.⁵ The result is a stable B-form structure throughout 5 ns of trajectory (Figure 2A); the dynamical structure is presented in a series of snapshots in Figure 3.

Case 2. Starting Structure A-Form in Water. MD results on duplex d(CGCGAATTCGCG) starting from the A-form in TIP3P-water are characterized by a rapid A- to B-form interconversion, analogous to that described for d(CCAACGT-TGG).²¹ We do not see junctions during the transition. Rather,

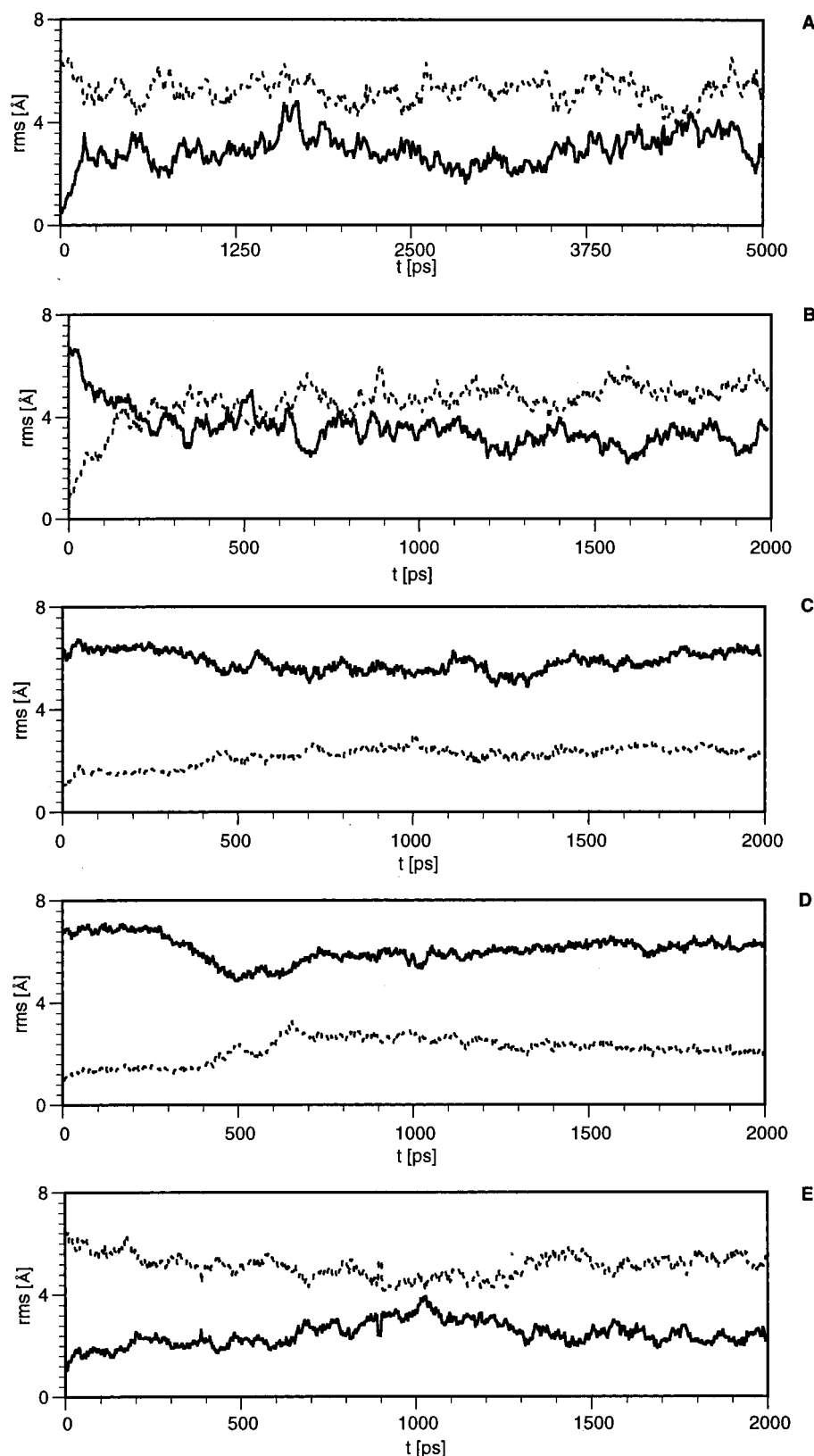


Figure 2. rms(A,t) (dotted line) and rms(B,t) (solid line) for the various systems studied. (A) The case 1 system (originally published in Young et al.⁵). (B) The case 2 system. (C) The case 3 system, biphasic OPLS-ethanol/TIP3P-water option. (D) The case 3 system, biphasic FK-ethanol/TIP3P-water option. (E) The case 4 system, again a biphasic OPLS-ethanol/TIP3P-water configuration option.

we see differing parameters convert to B-form at differing times. Examining the mechanism of the transition, sugar pucker and INC transition to B-form values within 500–750 ps. XDP converts from A to B values in the 750–1250 ps time range. The rms deviations of the MD structure with respect to A- and

B-canonical forms are nearly equal between 250 and 1100 ps (see Figure 2B). At greater than 1250 ps, rms(A,t) is greater than rms(B,t) (Figure 2B) and shows the MD structure to be closer to the B- than A-form. The A to B interconversion in water is complete by 1500 ps of MD. It is an average of the

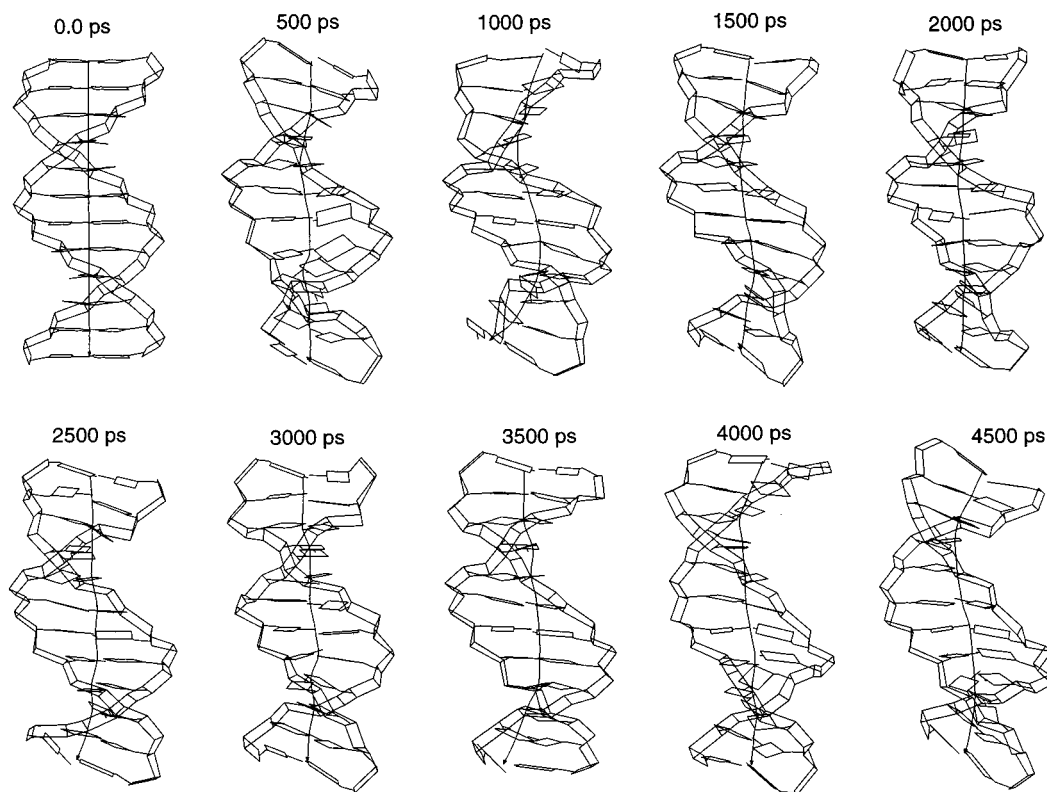


Figure 3. Snapshots of structures seen in the case 1 simulation (12Bw, see Table 1 for system details). The B-form is stable for greater than 4.5 ns in water.

TABLE 2: Average Values for Canonical DNA Forms and the Studied Ensembles

		XDP	INC	PHI
case 1	A-DNA canonical	-5.4	19	13
	B-DNA in water	-0.9 ± 0.50	-2.2 ± 8.0	130 ± 35
case 2	12Bw			
	A→B (last 500 ps) in water	-1.70 ± 0.50	1.93 ± 5.6	121 ± 39
case 3	12Aw			
	A-DNA in 85% opls-ethanol/water	-3.09 ± 0.61	13.9 ± 6.7	85.1 ± 60
	12Ae-ob			
case 4	A-DNA in 85% Fox-ethanol/water	-3.68 ± 0.61	20.0 ± 6.5	87.7 ± 90
	12Ae-fb			
	B-DNA in 85% opls-ethanol/water	-1.54 ± 0.50	2.79 ± 6.3	124 ± 40
	12Be-ob			
	B-DNA canonical	0.0	1.5	154

1500–2000 ps time range, which is presented in Table 2's statistics. Figure 4 presents the A to B structural conversion over the 2 ns simulation.

Case 3. Starting Structure A-Form, 85% (v/v) Ethanol/Water. In this phase of the project, we first examined the sensitivity of results to the form and parameters of the ethanol model. Simulations beginning with the A-form structure of d(CGCGAATTCGCG) were performed for both 85% (v/v) FK-ethanol/TIP3P-water and OPLS-ethanol/TIP3P-water. The initial configuration in both MD simulations was based on a random disposition of solvent molecules. MD on the A-form dodecamer structure in OPLS-ethanol remained essentially in the A-form based on XDP and INC over 2 ns of trajectory. However, in the equilibration segment of the FK-ethanol MD, the A-form structure d(CGCGAATTCGCG) melted in the central AATT base pairs. During this process, there was some hydrogen bonding between ethanols and the major groove atoms involved in the standard A•T base pairing.

This result prompted us to repeat the previous two simulations from an initial solvent configuration similar to that employed by Cheatham et al.,²⁰ with ethanol initially excluded from within

6 Å of the DNA. The results of MD should, in principle, be independent of the starting structure, but the purpose of equilibration phase of MD is to prepare the system in a form such that unphysical forces do not cause displacements that are beyond the radius of convergence of the numerical integrators. The rationale for the "biphasic" initial solvent structure is thus one of simply introducing the DNA to ethanol as gradually as possible. In this MD, the water and ethanol were observed to mix extensively during equilibration, but in the equilibrated solvent structure water molecules were predominant in the first solvation shell of the DNA. This equilibration protocol led the MD to a stable A-form of d(CGCGAATTCGCG) over 2 ns of trajectory for both the OPLS-ethanol and the FK-ethanol model, as evidenced by the rms deviations in Figure 2C,D. In both of these trajectories, INC and XDP for the dodecamer are clearly A-form, while the sugar puckers sample both the B-DNA C2'-endo conformation as well as the C3'-endo A-DNA conformation. The averages for INC, XDP, and pucker are presented in Table 2. In summary, once solvent equilibration is managed effectively, simulations at low water activity beginning with

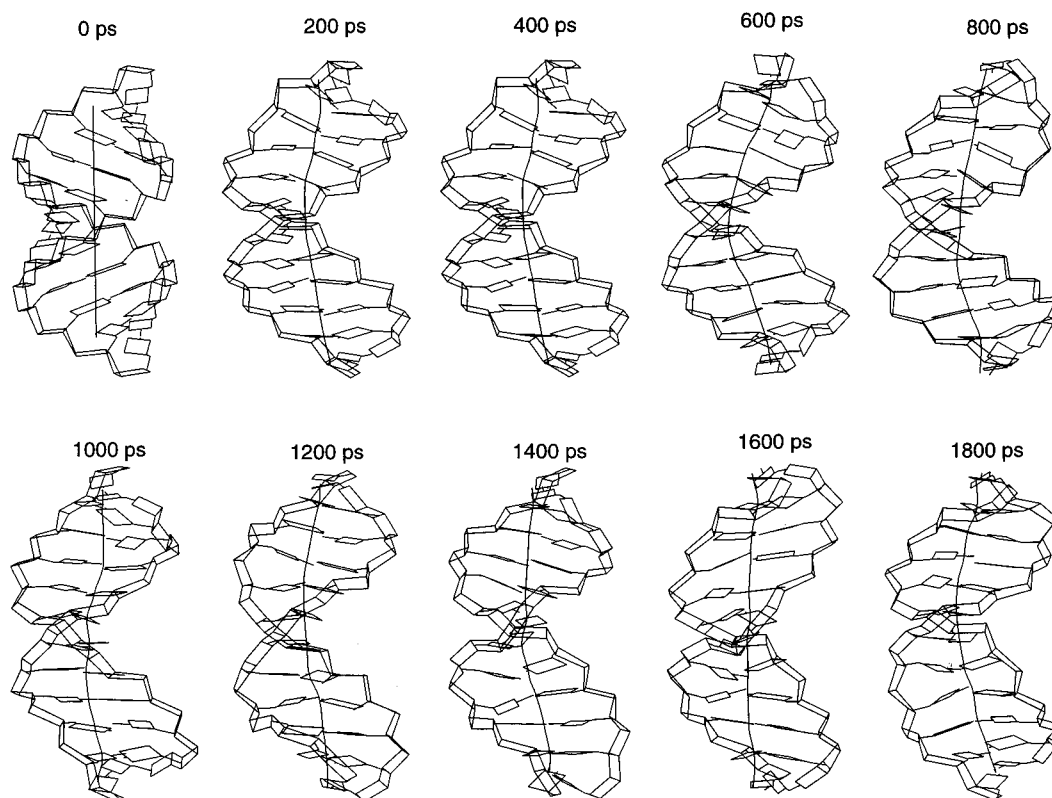


Figure 4. Snapshots of structures seen in the case 2 simulation (12Aw). The A-form converts to a B-form after 1500 ps in water.

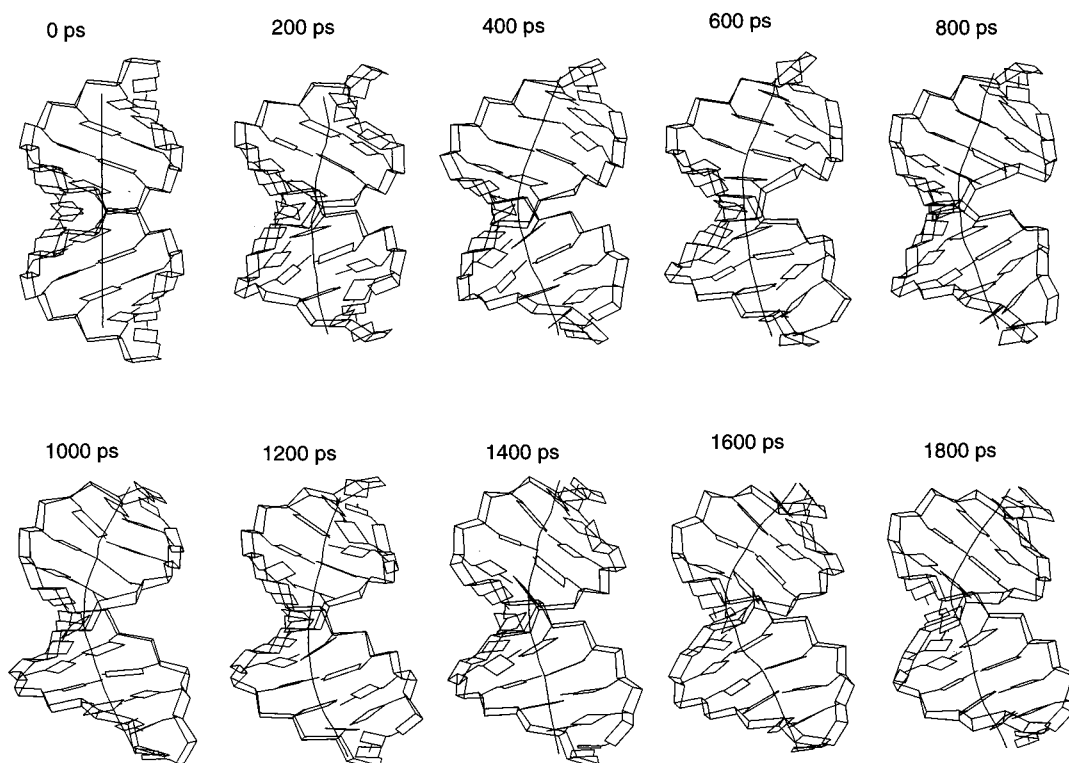


Figure 5. Snapshots of structures seen in the case 3, biphasic OPLS-ethanol/TIP3P-water option, simulation (12Ae-ob, see Table 1 for system details). The structures are A-form in 85% (v/v) ethanol/water for the 2 ns but show a pronounced kink in the central AATT base pairs.

A-form structures of the dodecamer remain A-form structures (Figure 5) and do not undergo A- to B-DNA conversions.

Case 4. Starting Structure B-Form in 85% (v/v) OPLS-Ethanol/Water. This MD was based on the OPLS-ethanol model and initiated from a biphasic solvent structure as described above. Solvent mixing was similar to that in the preceding case. In this case however, analyzed in Figure 2E,

the expected A to B interconversion was not observed and the DNA structure remains a B-form structure over the 2 ns time course of the simulation. Inspection of pucker, INC, and XDP likewise shows the B-DNA form (see Table 3).

Solvent Structure. We present here a comparison of the solvent structure around case 3 (A-DNA in 85% (v/v) ethanol/water) and case 1 (B-DNA in water). Analysis focuses on the

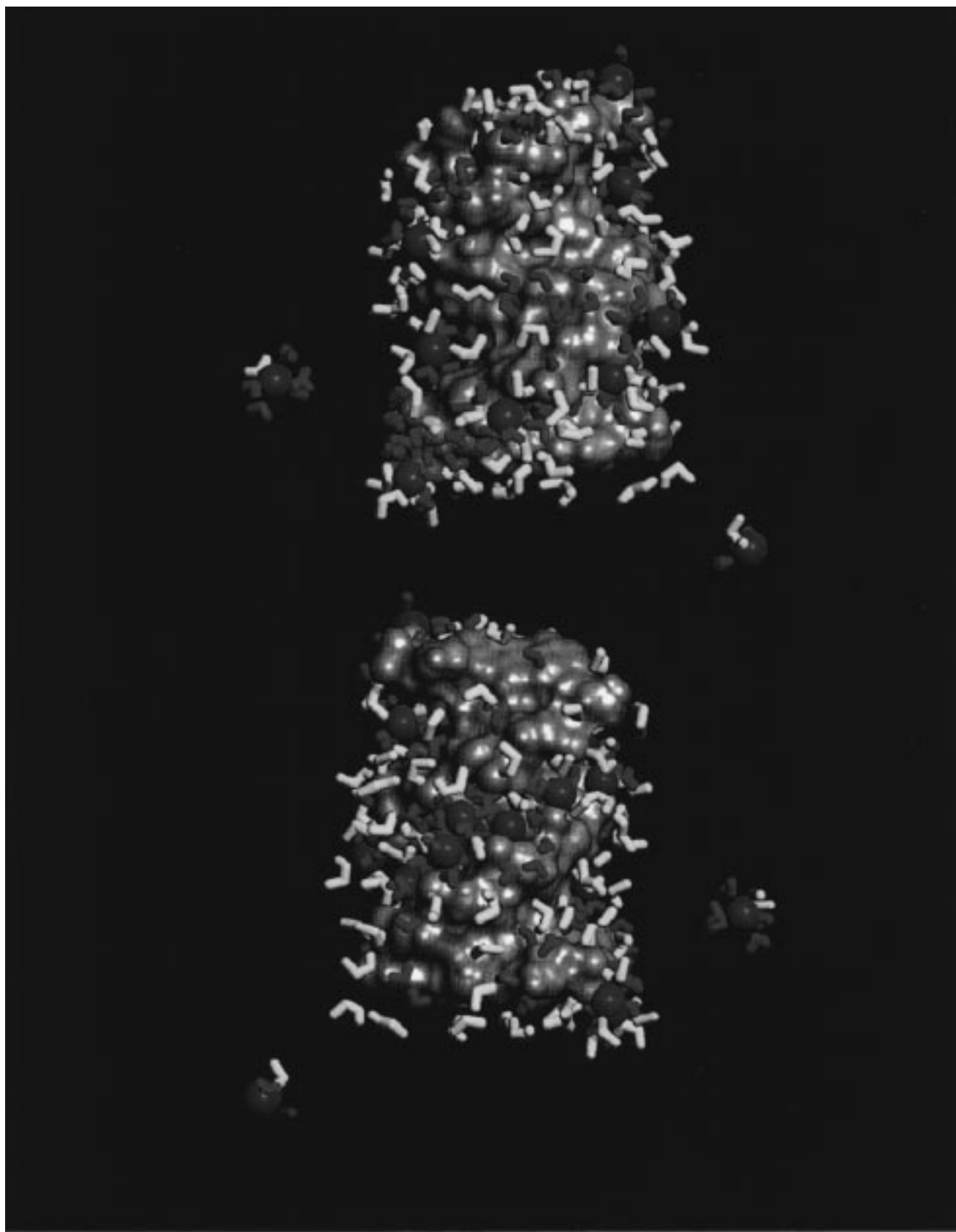


Figure 6. Snapshot of the 2000 ps structures from the A-DNA in 85% (v/v) ethanol/water (12Ae-ob, see Table 1 for system details). Top image is of the minor groove, and bottom image is of the major groove. The solvent-accessible surface of the DNA is shown in white. Na^+ ions are green, ethanols yellow, and waters cyan. Bulk waters are excluded for clarity.

distributions of water oxygens (OW), ethanol oxygens (OH), ethanol methyl atoms (C3), and Na^+ counterions (Na^+). For case 3, A-DNA in 85% (v/v) ethanol/water, all three solvent species, water, Na^+ , and ethanol, are found in the first solvation

layer around the DNA, where they make direct contacts with the DNA. This can be seen in the images of the system at 2000 ps shown in Figure 6. The DNA and the first solvation layer is shown, i.e., all solvent species less than 3.5 Å from the DNA.

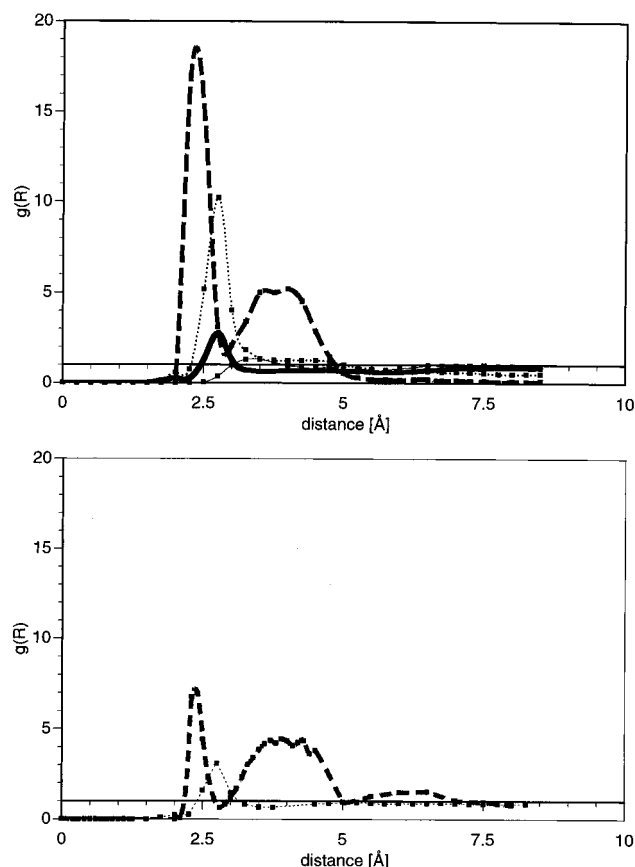


Figure 7. $g(R)$ for various atoms for A-DNA in 85% (v/v) ethanol/water (top) and B-DNA in water (bottom). Na^+ ions are shown by a dashed line. Water oxygen atoms are shown by a dotted line. Ethanol oxygen atoms are shown by a heavy solid line. Ethanol methyl group atoms are shown by a light solid line.

The first solvation layer around the B-DNA in case 1 is also comprised of members of all solvent species present, namely, both the water and the Na^+ ions.

A quantitative measure of the solvent distribution around the DNA shown in Figure 7 reveals some key differences between the distributions of the waters in the mixed solvent case (case 3) and those in the pure water simulation (case 1). In the pure water simulation, we see a distinct first solvation shell peak in the water oxygen radial distribution function, $g_{\text{OW}}(R)$, centered at 2.8 Å, with a density of roughly $3\times$ the average bulk density. The $g_{\text{OW}}(R)$ in this system converges to the bulk density at a distance roughly 5 Å from the surface of the DNA. For the mixed solvent simulation, however, the $g_{\text{OW}}(R)$ plot shows a much less homogeneous distribution of the water throughout the system. The vast majority of the water in this system is found concentrated in close proximity to the DNA, and a very low water density is found greater than 5 Å from the surface. The 2.8 Å OW first solvation layer peak in the mixed solvent case has a peak density greater than $10\times$ the average bulk density of waters in the system, a value more than $3\times$ the relative density of this peak in the pure water case. Thus, we find that the water in the 85% ethanol/water system equilibrates itself close to the relatively polar surface of the DNA as opposed to homogeneously mixing throughout the system.

The $g_{\text{Na}}(R)$ of the Na^+ ions in the two systems largely mirrors the trend in the water distributions. The vast majority of the Na^+ ion density in the mixed solvent case is located in very close proximity to the A-form DNA, and the distribution of the Na^+ ion density in the pure water case is much more homogeneous. The density of Na^+ ions located greater than 5

Å from the DNA surface is almost negligible in the mixed solvent simulation, partly a consequence of the fact that the density of ions found in the 2.4 Å first peak is nearly $20\times$ the average bulk value. By contrast, the $g_{\text{Na}}(R)$ in the pure water simulation converges to unity as R increases, indicative of a homogenized bulk distribution. The second broad $g_{\text{Na}}(R)$ peak is roughly comparable in both simulations.

The ethanol C3 and OH atom distributions for the case 3 simulation indicate that both atom types are present in the primary solvation layer of the DNA and participate in direct interactions with the DNA. The primary solvation layer density peaks are at 3.4 Å for the C3 atoms and at 2.8 Å for the OH atoms. The $g(R)$ for both atom types taper off to bulk value after 5–6 Å. The first peak in the ethanol oxygen atom $g(R)$ is at the same distance as the water oxygen peak. What is different between the two first shell peaks is that the OH peak height is roughly $3\times$ its bulk value, where the OW peak is greater than $10\times$ bulk. The absolute population of ethanol oxygen atoms found in the DNA primary solvation layer is 35–45% the total number of water oxygen atoms, despite the fact that the ethanols outnumber the waters. The $g_{\text{OH}}(R)$ density dips below unity at 3.0 Å and then begins to approach unity as distance increases. The ethanol methyl group atoms have a slight, broad peak at 3.5 Å. Afterward, their density remains close to bulk.

Discussion

This MD model of d(CGCGAATTCGCG) has a stable B-form structure in aqueous solution. The A-form of this sequence in aqueous solution interconverts to the B-form during equilibration, indicating that the A-form of d(CGCGAATTCGCG) is apparently not a stable structure at high water activity and the B-form is readily accessible from A-DNA regions of conformational space. The MD simulations in 85% ethanol, i.e., low water activity, indicate that both A- and B-forms of d(CGCGAATTCGCG) are stable structures for the model system. The results for the A-form are consistent with the expected behavior,^{13,15} but the lack of the B to A conversion in the MD for the low water activity system (case 4) is contrary to experimental expectations. This indicates that the system has a barrier to the B to A interconversion, and either the trajectory has not yet encountered the transition state in the potential surface, or the force field has a slight but significant overestimate of the stability of B-form structure. We carried out some exploratory MD simulations at an arbitrary elevated temperature of ~ 500 K in 85% OPLS-ethanol/TIP3P-water, but the simulations did not show either an A to B nor a B to A transition for d(CGCGAATTCGCG), a result that favors the latter explanation. Flatters et al.⁴⁴ have recently shown that MD based on the Cornell et al. force field shows an A-like conformation for the regions of the TATA box sequence in accord with experiment; thus the effect is subtle. The Cornell et al. force field¹ has thus far been more successful to date on DNA than the current CHARMM alternative,²⁸ which shows A-DNA independent of sequence or conditions.^{22–24,45}

Langley⁴⁵ has in progress an extensive study of this problem based on MD simulations on a DNA hexamer. His analysis for Cornell et al.¹ based simulations links the preferential stabilization of B-form structures to a slight skew in the distribution of sugar puckers and exocyclic χ parameters as compared with crystal structure data. He has designed a hybrid force field in which parameters for DNA were recursively altered to reproduce the crystallographically observed dihedral distribution for the backbone. The revised force field shows

improved behavior in describing A/B conformational preferences for a hexamer, and further studies are under way to determine the general applicability of this model.

The reasons that A-DNA is stable for the Cornell et al.¹ force field in low water activity are not unequivocally established at this point. The explanation offered by Cheatham et al.²⁰ is that hydration of the minor groove stabilizes B-DNA and hydration of the major groove stabilizes A-DNA. Inspection of Figure 6 and other snapshots from the case 3 simulation does show water and Na⁺ in the major groove. Whether this is cause or effect is hard to determine. An analysis of solvent accessibility⁴⁶ shows that A-DNA has roughly a 10% larger hydrophobic surface than B-DNA due to the exposure of sugars. This leads to an "oil drop" model for the A to B transition, where the sugar groups are squeezed into the interior of the helix (the B-DNA form), at high water activity due to the hydrophobic effect. However, the corresponding A/B tie line in the phase diagram determined from CD measurements shows little sensitivity to temperature,^{13,15} contrary to predicted inverse temperature dependence of a process driven predominantly by the hydrophobic effect.

MD structures from the simulations described above have subsequently been taken as the basis for a further study of the conformational free energies of the A- and B-forms of DNA.⁴⁷ Some 100 structures were culled from each MD and subjected to post facto free energy calculations. For the intramolecular components, enthalpies were obtained from calculations based on the Cornell et al. force field,¹ pooling the effects of DNA and counterions separately. Entropies were computed using the cross-correlation matrix of atomic displacements using the quasiharmonic method. Estimates of the free energy of solvation were obtained using the generalized Born theory with the modifications suggested by Jayaram et al.⁴⁸ and parameters developed for consistency with the AMBER charges.⁴⁹ The conformational preferences expected from experiment were faithfully reproduced in the calculations, but the magnitudes of the free energies are small and the result of large competing terms. Analysis of the results indicates that the molecular origins of the conformational preferences of A- and B-DNA lie in the differential effects of counterion condensation and solvation. For the A-form, the more compact structure and higher charge density results in a correspondingly more compact complexation of counterions, resulting in a lower intramolecular free energy for A- compared with the B-form. The B-form, a more open structure, is favored by hydration. In 85% ethanol/water, the solvation free energy is relatively low, and the intramolecular effects dominate, leading to a preference for the A-form. In water, the solvation term is larger and stabilizes the B-form. Full details of these calculations are provided in ref 47. The subtle balance of thermodynamics associated with explicit organization of mobile counterions around DNA played off against hydration effects is likely to be an important general feature in conformational preferences and fine control of structure in DNA and RNA systems.

Acknowledgment. This research was supported by Grant GM-37909 from the National Institute of General Medical Studies. D.S. thanks the NIH for NRSA fellowship GM-18117. The authors thank D. R. Langley and Prof. B. Jayaram for insightful remarks and Ms. J. McConnell for editorial assistance. We thank T. Cheatham, P. A. Kollman, and M. Crowley for advance releases of the AMBER code and preprints of their work. This work employed the computer resources of the PSC and the NCSA.

References and Notes

- (1) Cornell, W. D.; Cieplak, P.; Bayly, C. I.; Gould, I. R.; Merz, K. M.; Ferguson, D. M.; Spellmeyer, D. C.; Fox, T.; Caldwell, J. W.; Kollman, P. A. *J. Am. Chem. Soc.* **1995**, *117*, 5179–5197.
- (2) Pearlman, D. A.; Case, D. A.; Caldwell, J. W.; Ross, W. S.; Cheatham, T. E.; DeBolt, S.; Ferguson, D.; Seibel, G.; Kollman, P. *Comput. Phys. Commun.* **1995**, *91*, 1.
- (3) Cheatham, T. E., III; Miller, J. L.; Fox, T.; Darden, T. A.; Kollman, P. A. *J. Am. Chem. Soc.* **1995**, *117*, 4193–4194.
- (4) Darden, T.; York, D.; Pedersen, L. J. *Chem. Phys.* **1995**, *98*, 10089–10092.
- (5) Young, M. A.; Ravishanker, G.; Beveridge, D. L. *Biophys. J.* **1997**, *73*, 2313–2336.
- (6) Drew, H. R.; Wing, R. M.; Takano, T.; Broka, C.; Tanaka, S.; Itakura, K.; Dickerson, R. E. *Proc. Natl. Acad. Sci. U.S.A.* **1981**, *78*, 2179–2183.
- (7) Drew, H. R.; Dickerson, R. E. *J. Mol. Biol.* **1981**, *151*, 535–556.
- (8) Dickerson, R. E.; Drew, H. R. *J. Mol. Biol.* **1981**, *149*, 761–786.
- (9) Drew, H. R.; Samson, S.; Dickerson, R. E. *Proc. Natl. Acad. Sci. U.S.A.* **1982**, *79*, 4040–4044.
- (10) Fratini, A. V.; Kopka, M. L.; Drew, H. R.; Dickerson, R. E. *J. Biol. Chem.* **1982**, *257*, 14686–707.
- (11) Wing, R. M.; Drew, H. R.; Takano, T.; Broka, C.; Tanaka, S.; Itakura, I.; Dickerson, R. E. *Nature* **1980**, *287*, 755–758.
- (12) Lane, A.; Jenkins, T. C.; Brown, T.; Neidle, S. *Biochemistry* **1991**, *30*, 1372–1385.
- (13) Ivanov, V. I.; Minchenkova, L. E.; Minyat, E. E.; Frank-Kamentskii, M. D.; Schyolkina, A. K. *J. Mol. Biol.* **1974**, *87*, 817–833.
- (14) Basham, B.; Schroth, G. P.; Ho, P. S. *Proc. Natl. Acad. Sci. U.S.A.* **1995**, *92*, 6464–6468.
- (15) Ivanov, V. I.; Minchenkova, L. E.; Schyolkina, A. K.; Poletayev, A. I. *Biopolymers* **1973**, *12*, 98–110.
- (16) Fedoroff, O. Y.; Salazar, M.; Reid, B. R. *J. Mol. Biol.* **1993**, *233*, 509–572.
- (17) Saenger, W. *Principles of Nucleic Acid Structure*; Springer-Verlag: New York, 1984.
- (18) Kim, Y.; Geiger, J. H.; Hahn, S.; Sigler, P. B. *Nature* **1993**, *365*, 512–520.
- (19) Kim, J. L.; Nikolov, D. B.; Burley, S. K. *Nature* **1993**, *365*, 520–527.
- (20) Cheatham, T. E., III; Crowley, M. F.; Fox, T.; Kollman, P. A. *Proc. Natl. Acad. Sci. U.S.A.* **1997**, *94*, 9626–30.
- (21) Cheatham, T. E., III; Kollman, P. A. *J. Mol. Biol.* **1996**, *259*, 434–444.
- (22) Feig, M.; Pettitt, B. M. *J. Phys. Chem.* **1997**, *101*, 7361–7363.
- (23) MacKerell, A. D. J. *J. Phys. Chem.* **1997**, *101*, 646–650.
- (24) Yang, Y.; Pettitt, B. M. *J. Phys. Chem.* **1996**, *100*, 2564–2566.
- (25) van Gunsteren, W. F.; Berendsen, H. J. C. *Angew. Chem., Int. Ed. Engl.* **1990**, *29*, 992–1023.
- (26) McCammon, A. J.; Harvey, S. C. *Dynamics of Proteins and Nucleic Acids*; Cambridge University Press: Cambridge, 1986.
- (27) Beveridge, D. L.; Swaminathan, S.; Ravishanker, G.; Withka, J. M.; Srinivasan, J.; Prevost, C.; Louise-May, S.; Langley, D. R.; DiCapua, F. M.; Bolton, P. H. In *Water and Biological Molecules*; Westhof, E., Ed.; The Macmillan Press, Ltd.: London, 1993; pp 165–225.
- (28) Mackerell, A. D., Jr.; Wiorkiewicz-Kuizera, T.; Karplus, M. *J. Am. Chem. Soc.* **1995**, *117*, 11946–11975.
- (29) Duan, Y.; Wilkosz, Crowley, M.; Rosenberg, J. M. *J. Mol. Biol.* **1997**, *272*, 553–572.
- (30) Nornberg, J.; Nilsson, L. *J. Chem. Phys.* **1996**, *105*, 6052–6057.
- (31) Mooers, B. H.; Schroth, G. P.; Baxter, W. W.; Ho, P. S. *J. Mol. Biol.* **1995**, *249*, 772–784.
- (32) Arnott, S.; Campbell-Smith, P. J.; Chandrasekaran, R. In *CRC Handbook of Biochemistry and Molecular Biology*, Vol. 2; Fasman, G., Ed.; CRC Press: Cleveland, 1976; pp 411–422.
- (33) Pearlman, D. A.; Case, D. A.; Caldwell, J. W.; Ross, W. S.; Cheatham, T. E., III; Ferguson, D. M.; Seibel, G. L.; Singh, U. C.; Weiner, P.; Kollman, P. 4.1 ed.; UCSF: San Francisco, CA, 1995.
- (34) Jorgensen, W. L. *J. Am. Chem. Soc.* **1981**, *103*, 345–350.
- (35) Jorgensen, W. L. *J. Am. Chem. Soc.* **1981**, *103*, 341–345.
- (36) Jorgensen, W. L. *J. Am. Chem. Soc.* **1981**, *103*, 335–340.
- (37) Fox, T.; Kollman, P. A. Preprint, 1997.
- (38) Jorgensen, W. L. *J. Phys. Chem.* **1986**, *90*, 1276–1284.
- (39) Cieplak, P.; Cornell, W. D.; Bayly, C.; Kollman, P. A. *J. Comput. Chem.* **1995**, *16*, 1357–1377.
- (40) Bayly, C. I.; Cieplak, P.; Cornell, W. D.; Kollman, P. A. *J. Phys. Chem.* **1993**, *97*, 10269–10280.
- (41) Ravishanker, G. Wesleyan University, Middletown, CT, 1991.
- (42) Mehrotra, P. K.; Beveridge, D. L. *J. Am. Chem. Soc.* **1980**, *102*, 4287–4294.

- (43) Mezei, M.; Beveridge, D. L. *Methods Enzymol.* **1986**, 127, 21–47.
- (44) Flatters, D.; Young, M. A.; Beveridge, D. L.; Lavery, R. *J. Biomol. Struct. Dyn.* **1997**, 14, 1–8.
- (45) Langley, D. R. Manuscript in preparation.
- (46) Alden, C. J.; Kim, S. H. *J. Mol. Biol.* **1979**, 132, 411–434.
- (47) Jayaram, B.; Sprous, D.; Young, M. A.; Beveridge, D. L. *J. Am. Chem. Soc.*, submitted.
- (48) Jayaram, B.; Liu, Y.; Beveridge, D. L. *J. Chem. Phys.*, in press.
- (49) Jayaram, B.; Sprous, D.; Beveridge, D. L. *J. Phys. Chem.*, submitted.